Implementation and Experiments of Passive Set-Position Modulation for Internet Teleoperation and Slow/Varying-Rate Haptics

Ke Huang and Dongjun Lee

Abstract— In previous papers we proposed passive set-position modulation (PSPM) framework which enables us to connect continuous-time robot's position to a sequence of discrete set-position signals via spring coupling with damping injection while enforcing passivity. In this paper we present experimental results to show its stability and performance. We will also discuss some practical implementation details.

I. INTRODUCTION

In some teleoperation applications, the system needs to be operated over imperfect communication network (with constant/varying delay and packet loss: e.g. Internet). Surveillance, telesurgery [1] and exploration [2] are instances of these applications. In addition, in some haptic simulation systems with complex virtual environment (e.g. deformable object with multipoint contact [3]), the update-rate from the virtual world can be much slower w.r.t. the device servo-rate and possibly varying.

In previous papers [4], [5], we showed that the major problem of the instability caused by imperfect communication and slow virtual environment (VE) is that the received discrete-time set-position signals may be too aggressive (e.g. huge jump). This kind of jump may generate energy which breaks the passivity of the closed-loop system. To solve this "jump" problem, we proposed **passive set-position modulation (PSPM)** in [4], [5]. The key idea of PSPM is to modulate the aggressive discrete set-position data and provide the local robot a passivity-enforcing set-position signal sequence. By using this modulated set-position signals for the local spring-damper controller, the closed-loop system can be guaranteed to be energetically passive.

For the passivity-based teleoperation control with time delays, several important results have been proposed so far. In [6], the scattering-based method was presented. This method can passify the communication block. Hence the passivity of the closed-loop system can be achieved. A further extension to scattering-based method is *wave variables* [7]. The work in [8] showed that for teleoperator using PD control, enough local damping can make the system passive. However, the methods in [6]-[8] can only handle constant time delays. In [9], a modified scattering-based method was proposed to deal with time-varying delays. Nevertheless, this method [9] requires the knowledge of time delays. All of the results in [6]-[9] also require the communication block to be

continuous which is not true for some communication links (e.g. Internet).

For stable haptic interaction control, virtual coupling [10] provides a way to passively connect haptic device and the VE. However, the virtual coupling parameters (virtual stiffness and damping) are restricted by the device damping and the simulation update rate. For a given haptic device, if the update rate is slow, the virtual coupling parameters may become so small that the system may not achieve good performance. Moreover, the virtual coupling cannot work for the VE with varying update rate. In [11], passivity observer (PO) and passivity controller (PC) are proposed to insure the passivity of a haptic interaction system. But the noisy behavior of PO/PC at low velocity is a well-known problem [12]. Furthermore, the PO/PC is derived for discrete system, but the haptic interaction system is hybrid (i.e. continuous haptic device and discrete VE), although some attempts have been made to address this issue [13].

The rest of the paper is organized as follows. The PSPM framework and its properties are reviewed in Sec. II. Experimental results are presented in Sec. III and IV to show the properties of PSPM, and Sec. V contains the conclusions.

II. PASSIVE SET-POSITION MODULATION

Consider an n-degree-of-freedom (n-DOF) nonlinear robotic system,

$$M(x)\ddot{x} + C(x,\dot{x})\dot{x} = \tau + f \qquad (1)$$

where $M(x) \in \Re^{n \times n}$ is the inertia matrix, $C(x,\dot{x}) \in \Re^{n \times n}$ is the Coriolis matrix. $x \in \Re^n$ is the position and $\tau \in \Re^n$ is the control torque. This robotic system is interacting with human or environment through the power port $f^T \dot{x}$, where $f \in \Re^n$ and $\dot{x} \in \Re^n$ are the interaction force and velocity.

In many teleoperation and haptics applications, the position tracking between the master and slave is required. For this, the most common way in practice is to connect $x(t) \in \Re^n$ and the set-position signal $y(k) \in \Re^n$ via a local spring-damper control:

$$\tau(t) = -B\dot{x}(t) - K(x(t) - y(k)) \qquad (2)$$

where $B, K \in \Re^{n \times n}$ are diagonal matrices which represent damping and spring matrices respectively, and $y(k)$ is the set-position data received at each reception time $t_k (k = 1, 2, 3...)$.

Consider the robot system (1) with control (2), and $y(k)$ is transmitted through imperfect communication network. The delay for each packet may be varying. Thus, there is no guarantee that $y(k)$ is sent before $y(k+1)$ from the sending port. Due to this, some packets are *time-swapped* during transition.

In addition to time-swapping, some communication network (e.g. wireless network) also causes the loss of packets. The delay and packet-loss are two major reasons of aggressive set-position signal sequence. This aggressive signal sequence may cause passivity-breaking spring energy jump which can be presented as,

$$\Delta P(k) := \frac{1}{2}||x(t) - y(k)||_K^2 - \frac{1}{2}||x(t^-) - y(k-1)||_K^2 \quad (3)$$

If $\Delta P(k) > 0$, it is passivity-breaking because the discrete set-position data switching generates positive energy which can be injected into the robot system.

To solve this energy jumping problem, we proposed PSPM framework in [4], [5]. The key idea is to modulate the aggressive set-position signal and provide the local robot a passivity-enforcing set-position signal sequence. By using the modulated set-position signal sequence, the energy jumping is modulated and compensated by the system's available energy. The complete PSPM algorithm is listed below. In the algorithm, $E(k)$ is the virtual energy reservoir; $D_{\min}(k)$ refers to the estimation of damping dissipation during $I_k := [t_k, t_{k+1})$; $\bar{y}(k)$ is the modulated set-position signal; $\Delta \bar{P}(k) := \bar{\varphi}(t_k) - \bar{\varphi}(t_k^-) = \frac{1}{2}||x(t_k) - \bar{y}(k)||_K^2 - \frac{1}{2}||x(t_k^-) - \bar{y}(k-1)||_K^2$ is the modulated spring energy jump; $\Delta E_y(k)$ (or $\Delta E_x(k)$, resp.) is the energy shuffling term received from (or to be sent, resp.) the communication. For better understanding of the PSPM algorithm, Fig. 1 is given to show the system structure and the energy flow among the damping dissipation B, virtual energy reservoir $E(k)$ and PSPM block.

Algorithm 1 Passive Set-Position Modulation

1: $\bar{y}(0) \Leftarrow x(0), E(0) \Leftarrow \bar{E}, k \Leftarrow 0$
2: **repeat**
3:     **if** data $(y, \Delta E_y)$ received **then**
4:         $k \Leftarrow k+1$
5:         $y(k) \Leftarrow y, \Delta E_y(k) \Leftarrow \Delta E_y$
6:         retrieve $x(t_k), x_i^{\max}(k-1), x_i^{\min}(k-1)$
7:         find $\bar{y}(k)$ by solving

$$\min_{\bar{y}} ||y(k) - \bar{y}(k)||$$
$$E(k) \Leftarrow E(k-1) + \Delta E_y(k) + D_{\min}(k-1) - \Delta \bar{P}(k) \geq 0$$
$$(4)$$

8:         **if** $E(k) > \bar{E}$ **then**
9:             $\Delta E_x(k) \Leftarrow E(k) - \bar{E}, E(k) \Leftarrow \bar{E}$
10:        **else**
11:            $\Delta E_x(k) = 0$
12:        **end if**
13:        send $(x(t_k), \Delta E_x(k))$ or discard if no counterpart
14:    **end if**
15: **until** operation terminated

The optimization problem (4) is the key part of the algorithm. By the optimization objective, $\bar{y}$ is pushed to y as close as possible yet only to the extent permissible by the available energy in the system (i.e. $E(k-1) + \Delta E_y(k) + D_{\min}(k-1)$).
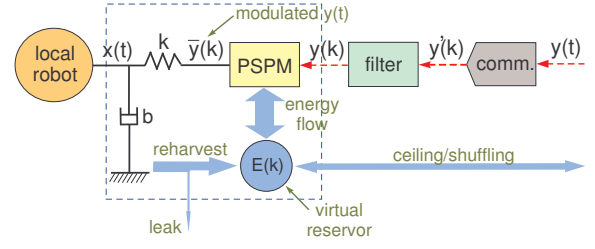

Fig. 1.   Energetics of the PSPM

This available energy is used to compensate the modulated energy jumping $\Delta \bar{P}$.

As presented in (4) and Fig. 1, the damping dissipation through B in (2) is recycled by $D_{min}(k)$ which is computed as,

$$D_{\min}(k) := \frac{1}{t_{k+1} - t_k} \sum_{i=1}^{n} b_{ii}(x_i^{\max}(k) - x_i^{\min}(k))^2 \quad (5)$$

where b_{ii} is the diagonal elements of B, and $x_i^{\max}, x_i^{\min}$ represent the maximum and minimum of the i-th element of $x(t)$ during I_k. Note that this computation is based on position signals, so the error caused by numerical differentiation/integration can be avoided. Following from [4], $D_{\min}(k) \leq D(k), \forall k \in \mathbb{N}$, where $D(k) := \int_{t_k}^{t_{k+1}} \dot{x}^T(t) B \dot{x}(t) dt$ is the actual damping dissipation. This result is important because if not, extra energy (i.e. $D_{min}(k) - D(k)$) can be generated and enter the virtual energy reservoir, resulting in the violation of passivity. From another point of view, because E provides energy to push $\bar{y}(k)$ to $y(k)$, the level of E is directly related to the performance. Therefore, we want $D_{min}(k)$ to be close to the real dissipation $D(k)$. From [4], this *energy re-harvesting error* can be written as,

$$\sum_{k=1}^{N} (D(k) - D_{\min}(k)) \approx \frac{1}{3} a_{max}^2 \bar{\sigma}[B](t_N - t_0)\Delta t^2 \quad (6)$$

where a_{max} is the maximum acceleration; $\bar{\sigma}[B]$ is the maximum singular value of B; t_N is the update time at N^{th} step; and Δt is the averaged update time interval. From (6), we can see the energy reharvesting error is quadratically reduced as we increase the update rate Δt. Thus, by accelerating the update rate, $D_{min}(k)$ becomes closer to the real dissipation $D(k)$ and the performance can be improved. The update rate can be accelerated by any data interpolation methods. In this paper, we use low-pass filtering to achieve this.

The *energy shuffling* terms $\Delta E_y(k), \Delta E_x(k)$ are designed to emulate master-slave energy coupling. The energy shuffling is initiated when the energy level in the virtual energy reservoir touches the energy ceiling $\bar{E}$ (see Line 9 of Algo. 1). Here, the energy ceiling $\bar{E}$ is designed to prohibit the excessive energy accumulation in the virtual energy reservoir.

Throughout the rest of this paper, we will use $\star_1, \star_2$ or $\star^1, \star^2$ to represent the master and slave variables respectively.

The PSPM algorithm possesses the properties which are important for teleoperation and haptic applications. The properties are: 1) the closed-loop system is energetically
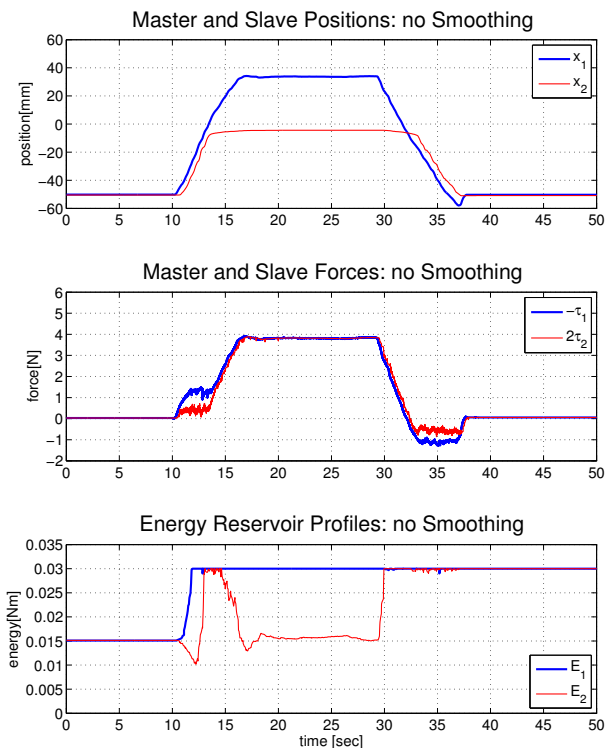
Fig. 2.   Teleoperation without low-pass filtering.

Fig. 3.   Teleoperation with low-pass filtering.

passive and stable; 2) the master and slave will coordinate with each other ($x_1(t) \rightarrow x_2(t)$) if the virtual energy reservoirs are not empty and both sides are released; and 3) The slave force is reflected to the human operator (i.e. $f_1 = -K_1 K_2^{-1} f_2$). For more details, see [4].

III. EXPERIMENT: BILATERAL TELEOPERATION OVER INTERNET

In this section, the PSPM framework is applied to the bilateral teleoperation over the Internet. We perform three different experiments to show the properties of PSPM. We use a PHANTOM® Desktop™ as the master device and a PHANTOM® Omni™ as the slave device. Both of them are connected to a PC running Windows XP®. In this paper, the experiments are performed in 1 degree-of-freedom (DOF): x-axis position of the device end-effector is measured and used as set-position signal. We believe this 1-DOF experiment is sufficient to show the PSPM properties and features, because, for the multi-DOF experiment, the result of each axis is very similar to the result of the 1-DOF experiment as presented here. An Internet-like communication network is simulated locally. The packets are sent from each side every 5ms. The delays of packets obey random distribution. In the experiments, the round-way delay varies from 0.2s to 1.4s. As aforementioned in Sec. II, the packets can be swapped due to the varying delays; we correct this by dropping the old data[1]. By this packet dropping, portion of the packets are lost (loss rate is 92.2% in the experiments) and a more

sparse signal sequence is produced. In the experiments, time intervals between two consecutive available packets is 106ms in average. This sparseness may lead to unsmooth perception. Therefore, a first-order low-pass infinite impulse filter (IIR) is placed before the PSPM block (see Fig. 1) to interpolate this sparse signal sequence. After the interpolation, the time interval between two successive packets becomes 5ms in the experiments. By using this interpolated signal sequence the perception become smoother. As shown by (6), the IIR will also improve the energy re-harvesting efficiency.

For the energy reservoir, we use $(E_1(0), \bar{E}_1, E_2(0), \bar{E}_2) = (0.015, 0.03, 0.015, 0.03)$Nm. The shuffling energy $\Delta E_y(k)$, $\Delta E_x(k)$ are sent along with set-position signals and be collected from all received packets at the other side even if swapped position data $y(k)$ are discarded. For the local controller, we use $(K_1, K_2) = (100, 50)$N/m, $(B_1, B_2) = (5, 5)$Ns/m.

In the first experiment, a standard contact experiment is performed on the system without/with IIR respectively (Fig. 2 and 3). A rigid wall is placed around 0mm. Both of the master and slave start at -50mm, then the operator holds the master device and moves to the right. After contacting with the wall, the operator keeps moving until the force is big enough to confirm the existence of wall. Then the master is moved back to its start position.

Both Fig. 2 and Fig. 3 show that the positions of the master and the slave are coordinated when both sides are released (0-10s and 40-50s in Fig. 2; 0-25s and 110-140s in Fig. 3). And the human can feel the two-times scaled contact force of the slave while contacting with the wall which is predicted

---

[1]Better packet pre-processing scheme may exist but the discussion about it is beyond the scope of this paper and will be pursed in our future work.
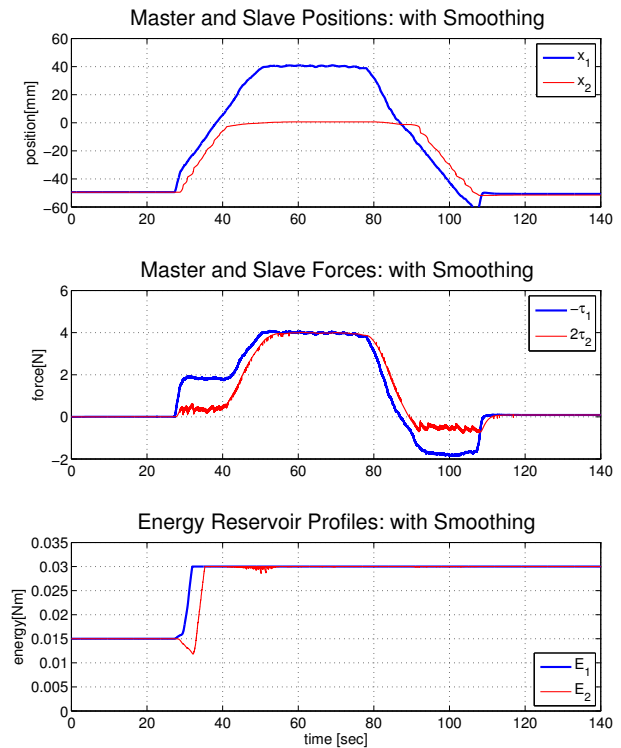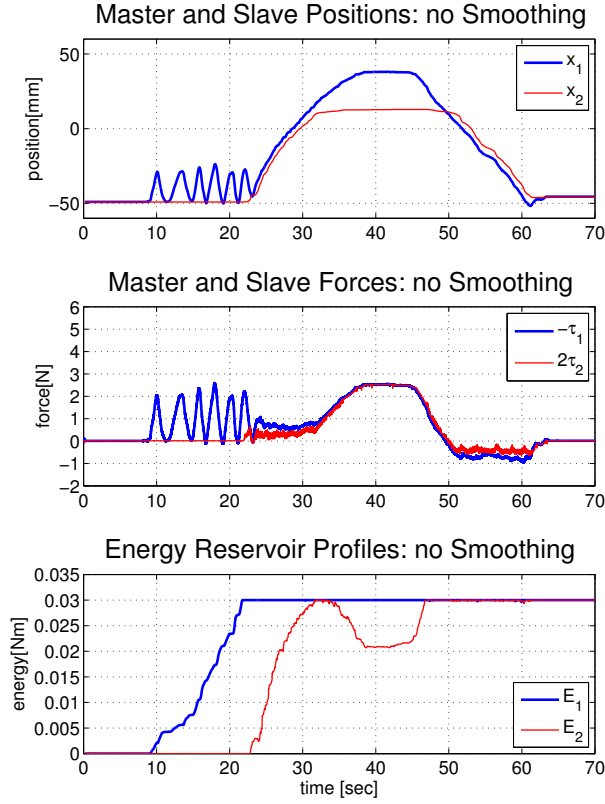
Fig. 4. Teleoperation starts with zero initial energy.

Fig. 5. Passifying/Stabilizing action of the PSPM for teleoperation.

by PSPM property (i.e. $f_1 = -K_1 K_2^{-1} f_2$).

The effects of low-pass filtering can be seen by comparing Fig. 2 and Fig. 3 (e.g. the motion is slower for the experiment using IIR). In Fig. 2, during the motion in free space, the jittering force perception can be observed (10s-15s, 33s-37s), which can distract the sense of immersion of the human operator. In Fig. 3, the human perception is smoothed by IIR (27s-42s, 90s-108s), yet, the extra delay (see the gap between x_1 and x_2) yields "heavier" experience (i.e. larger force during the motion in the free space). Comparing the virtual energy reservoir profiles in Fig. 2 and Fig. 3, with the IIR filtering, the energy re-harvesting efficiency is improved (e.g. E_2 has no significant drop in Fig. 3) as predicted by (6).

The *take-off* experiment (Fig. 4) is designed to show the energy coupling between the master and the slave. In the beginning, the slave does not move, since there is no available energy (i.e., $E_2(0) = 0$) to push $x_2(k)$. Yet, as shown in Fig. 4, as human injects energy, E_1 reaches to $\bar{E}$, and extra energy is shuffled to the slave side, thereby, allowing the slave to follow master position thenceforth.

The next *Passifying/Stabilizing* experiment (Fig. 5) is to show how PSPM passifies the teleoperator system by the set-position signal modulation. In this experiment, with both sides in free space (i.e. no contact forces), we try to make the teleoperator unstable by wildly shaking the master haptic device, then, releasing the master at 3.5s. Fig. 5 shows that the system is stabilized by the PSPM. We can see that the
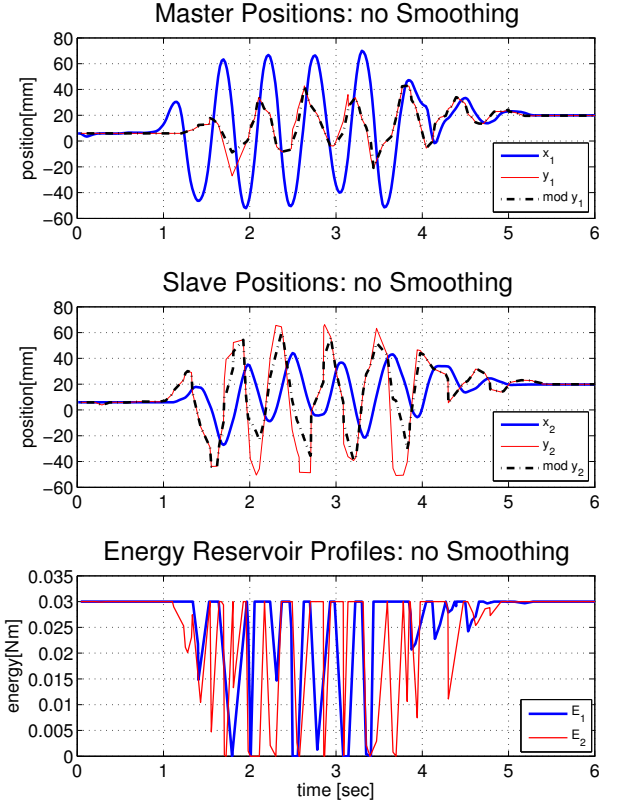
raw signals y_1, y_2 were modulated when they become too aggressive. When the PSPM is turned off, the aggressive position signal made the system unstable (not shown here).

IV. EXPERIMENT: SLOW AND VARIABLE-RATE HAPTICS

In this section we use PSPM to connect the haptic device with VE whose update rate is slow and varying. Following [5], in order to extend the PSPM to the discrete virtual world, we need the discrete simulation to be passive. In [14], we proposed a non-iterative passive numerical integrator which can enforce such discrete-time passivity of the simulation:

$$M_2 \frac{v_{k+1} - v_k}{T_k} + B_2 \frac{v_{k+1} + v_k}{2} + K_2 \left(\frac{x_{k+1} + x_k}{2} - \bar{y}_k \right) = f_k$$
$$\frac{v_{k+1} + v_k}{2} = \frac{x_{k+1} - x_k}{T_k} \quad (7)$$

where M_2 is the inertia matrix of the virtual slave; x_k, v_k are the position/velocity at update time t_k; and f_k is the environment force at t_k. Here, $T_k := t_{k+1} - t_k$, and $\bar{y}(k)$ is the modulated set-position signal of the haptic device.

Note in (7) that, a discrete spring-damper connection is employed between the virtual slave's position x_k and the modulated set-position signal $\bar{y}_k$. For the haptic device, we use the control (2) which is a spring-damper connection. Thus the slave side has the similar energetic structure as the master side, i.e., kinetic and spring energy. Because the discrete simulation is open-loop passive, the energy jump
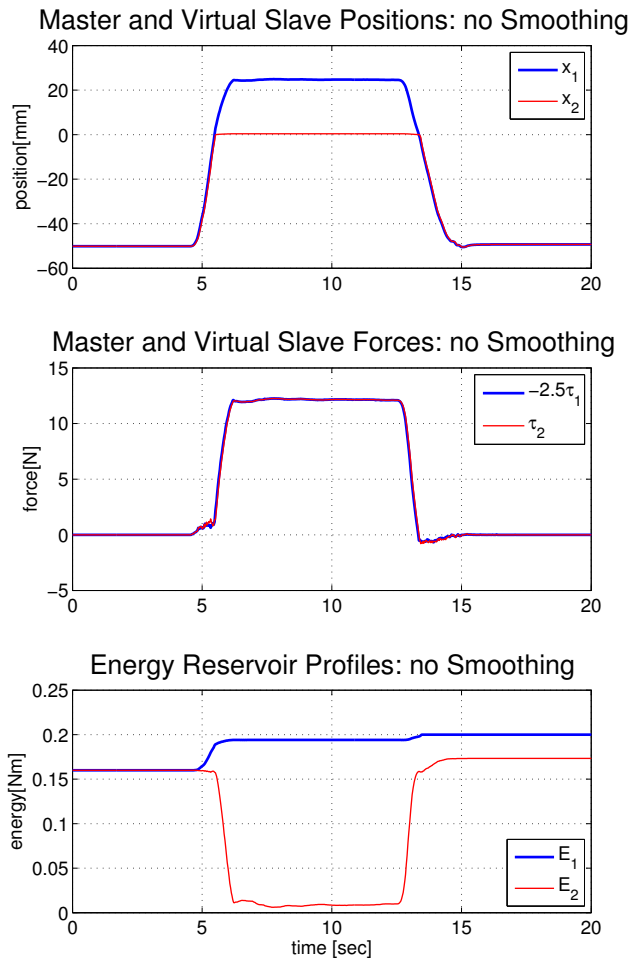
Fig. 6. Haptic interaction experiment with PSPM.

(caused by aggressive discrete set-position signal), similar to the master side, is the only way to break the passivity of the slave side. By using PSPM for the VE, this aggressive discrete set-position signal can also be modulated while enforcing passivity. By doing this, we can then achieve the 2-port hybrid passivity for the closed-loop system:

$$\int_0^{t_N} f^T(t)\dot{x}(t)dt + \sum_0^N f_k^T \hat{v}_k T_k \geq -d^2 \tag{8}$$

where $\hat{v}_k = \frac{v_{k+1}+v_k}{2}$.

For the haptic device, we use a PHANTOM® Desktop™ which is connected to a PC running Windows XP®. For the virtual world, a simple 1-DOF VE including a free space and a virtual wall is implemented using (7) in the same PC. The update rate of this VE is slowed down and varied. We use this simple VE because the virtual wall is a standard VE setting for haptic experiment [10]. Also, even if it is simple, we believe that it is sufficient to show the PSPM properties for the slow and varying update rate. The experiments are performed in 1-DOF because the result from each axis of multi-DOF experiment is very similar to the result of 1-DOF experiment.

The PSPM parameters in the following experiments are:

$(B_1, K_1, \bar{E}) = (5\text{Ns/m}, 200\text{N/m}, 0.2\text{Nm})$ for the device side; and $(B_2, K_2, \bar{E}) = (5\text{Ns/m}, 500\text{N/m}, 0.2\text{Nm})$, $M_2 = 0.001\text{kg}$ (i.e. mass of the virtual proxy), update rate is $10\text{ms} \leq T_k \leq 50\text{ms}$ for the VE. Force saturation on the haptic device is implemented by the manufacturer.

The first experiment is to show the position coordination and force reflection (see Fig. 6). Both of the device and virtual slave start at -50mm and then move towards the virtual wall (placed at 0mm). After coming into contact with the virtual wall, the human keeps moving until the feedback force is large enough to confirm the existence of the virtual wall. After that, the master moves back into the free space. From Fig. 6, the position coordination between the master and the slave is achieved if outside of the wall (0s-4.5s, 15.5s-20s). The force is reflected to the master side from the slave side during hard contact (6s-13s).

The second experiment (Fig. 7, 8) shows the passivity property of the PSPM. On the top of variable data update rate, we include the round-way communication delay between the haptic device and the VE that varies from 2.0s to 4.0s. At the beginning, the human operator gives an impulsive push to the haptic device and then releases it. This procedure is applied to the haptic systems without and with the PSPM. Without the PSPM, as shown in Fig. 7, we can observe wild oscillation of the master and the slave. Note that for the haptic system without the PSPM, the coupling between the haptic device and passive VE becomes similar to the virtual coupling [10]. Here, the control is saturated due to the force saturation of the device . If without this saturation, the system is expected to be even more unstable and eventually diverge. In contrast, from Fig. 8, it is clear that the haptic system with the PSPM maintains stability.

In Fig. 7, 8, if there is no communication delay and the update rate is uniform, the virtual coupling technique [10] can also enforce passivity of the combined system with properly chosen parameters (i.e. K_1, K_2, B_1, B_2). However, if the communication is not perfect (i.e. delayed and/or packet-loss) or the update rate is varying as done here, the virtual coupling in general can not ensure passivity. In contrast, the PSPM can still enforce passivity in this case. Moreover, since the PSPM enforces passivity separately for the continuous device and the discrete virtual world (with discrete-time passive integrator (7)) we can freely choose parameters for the virtual world (e.g. M_2, K_2, B_2 and virtual wall K, B). Of course, the PSPM assumes the device servo rate much faster than virtual world update rate. This assumption may not be true for high performance haptic simulation. For a result to relax this assumption, see [15].

V. CONCLUSIONS

In this paper, we review the PSPM framework which enables us to passively connect a master robot with a slave robot or a passive VE over discrete communication network with varying-delay and packet-loss. Then, we apply the PSPM to a bilateral teleoperation system via imperfect communication (i.e. varying-delayed and packet-loss), and experimentally show the properties of the PSPM. We also
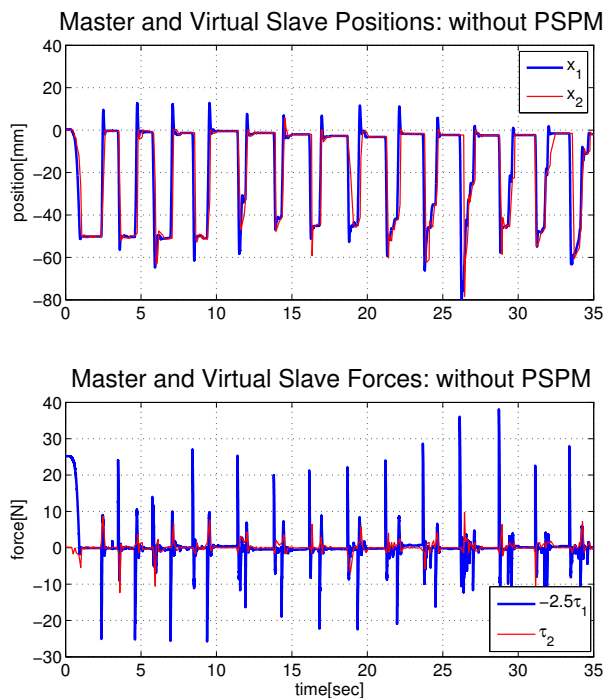
Fig. 7. Instable haptic interaction experiment without PSPM.

Fig. 8. Stable haptic interaction experiment with PSPM.

show the efficacy of the PSPM's energy coupling and data interpolation. The PSPM is also implemented for haptic interaction system with slow and varying VE and show the stability and performance properties of the PSPM.

REFERENCES

[1] J. Marescaux, J. Leroy, F. Rubino, M. Smith, M. Vix, M. Simone, and D. Mutter, "Transcontinental robot-assisted remote telesurgery: Feasibility and potential applications," Annals of Surgery, vol. 235, no. 4, p. 487, 2002.
[2] P. S. Schenker, T. L. Huntsberger, P. Pirjanian, E. T. Baumgartner, and E. Tunstel, "Planetary rover developments supporting mars exploration, sample return and future human-robotic colonization," Autonomous Robots, vol. 14, no. 2, pp. 103–126, 2003.
[3] J. Barbič and D. L. James, "Six-dof haptic rendering of contact between geometrically complex reduced deformable models," IEEE Transactions on Haptics, vol. 1, pp. 39–52, Jan.-June 2008.
[4] D. Lee and K. Huang, "Passive position feedback over packet-switching communication network with varying-delay and packet-loss," in Haptics Symposium, March 2008, pp. 335–342.
[5] ——, "Passive set-position modulation approach for haptics with slow, variable, and asynchronous update," in World Haptics Conference, 2009.
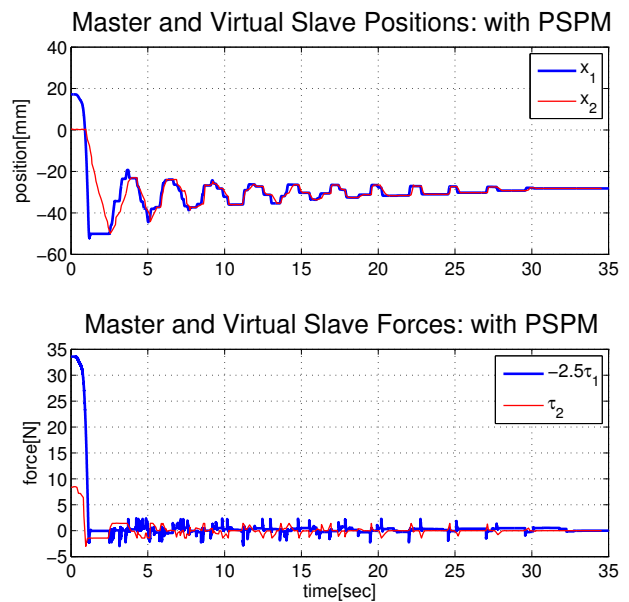[6] R. Anderson and M. Spong, "Bilateral control of teleoperators with time delay," IEEE Transactions on Automatic Control, vol. 34, no. 5, pp. 494–501, 1989.
[7] G. Niemeyer and J. Slotline, "Stable adaptive teleoperation," IEEE Journal of Oceanic Engineering, vol. 16, no. 1, pp. 152–162, 1991.
[8] D. Lee and M. Spong, "Passive bilateral teleoperation with constant time delay," IEEE Transactions on Robotics, vol. 22, no. 2, pp. 269–281, 2006.
[9] N. Chopra, M. Spong, S. Hirche, and M. Buss, "Bilateral teleoperation over the internet: the time varying delay problem," in American Control Conference, vol. 1, 2003.
[10] J. E. Colgate, M. Stanley, and J. Brown, "Issues in the haptic display of tool use," in Proc. IEEE/RSJ Int. Conf. On Intelligent Robotics and Systems, Pittsburgh, PA, 1995, pp. 140–145.
[11] B. Hannaford and J. Ryu, "Time domain passivity control of haptic interfaces," IEEE Transactions on Robotics and Automation, vol. 18, pp. 1–10, February 2002.
[12] J. H. Ryu, J. H. Kim, D. S. Kwon, and B. Hannaford, "A simulation/experimental study of the noisy behavior of the time domain passivity controller for haptic interface," in IEEE International Conference on Robotics and Automation, April 2005.
[13] J.-H. Ryu, Y. S. Kim, and B. Hannaford, "Sampled and continuous time passivity and stability of virtual environments," in IEEE Int. Conf. on Robotics & Automation, Taipei, Taiwan, September 2003.
[14] D. Lee and K. Huang, "On passive non-iterative varying-step numerical integration of mechanical systems for haptic rendering," in ASME Dynamic Systems & Control Conference, 2008, available at http://web.utk.edu/ djlee/papers/DSCC08b.pdf.
[15] D. Lee, "Extension of colgate's passivity condition for variable-rate haptics," in IEEE/RSJ Int'l Conf. on Intelligent Robots & Systems, 2009, to appear at http://web.utk.edu/~djlee/papers/IROS09a.pdf.